Journal of Constructional Steel Research 122 (2016) 292–307

Contents lists available at ScienceDirect

Journal of Constructional Steel Research

Investigation of CFS shear walls with one and two-sided steel sheeting

Nader K.A. Attari [a,*], S. Alizadeh [b], S. Hadidi [a]

[a] Department of Structural Engineering, Building & Housing Research Center, Tehran, Iran
[b] Department of Civil Engineering, Sharif University of Technology, Tehran, Iran

ARTICLE INFO

Article history:
Received 23 December 2015
Received in revised form 17 March 2016
Accepted 21 March 2016

Keywords:
Cold-Formed Steel
Steel shear walls
Steel sheeting
Shear wall capacity
FEM

ABSTRACT

In this study six Cold-Formed Steel shear wall (CFS) with one and two side steel sheeting are tested under reversed cyclic loading. Besides, thirteen numerical models are simulated, using nonlinear finite element method, and analyzed under monotonic pushover loading. The studied parameters are the comparison of one and two side steel sheeting, the nominal thickness of steel sheet and boundary elements, and height to width aspect ratios of the wall. The performance of tested specimens is investigated in terms of lateral load-story drift response, failure modes and ultimate strength of shear walls. Based on AISI S213 the available strength of two-sided steel-sheathed walls is cumulative but the results of the experimental study show that the capacity of two-sided steel-sheathed walls is more than twice of one side steel sheathed if the boundary elements are strong enough to sustain imposed forces. Overall, the performance of CFS shear walls is highly depending on the ratio of boundary element thickness to steel sheet thickness. According to numerical models, there is a linear relationship between the nominal sheet thickness and the ratio of ultimate strength to nominal frame thickness.

1. Introduction

Light-framed Cold-Formed Steel (CFS) structures have been introduced to construction industry in the middle of 40s, while, at that time using this type of structures has not been widely developed because of high constructional costs. During the early 90s utilizing of this system in low to medium-rise buildings has been increased such that using CFS structures were become very popular in many regions.

In CFS structures, CFS framed walls combined with structural wood, gypsum, cement boards or bracing systems provide the lateral resistance of the structure. Recently, utilizing CFS frames sheathed by thin steel plates as shear wall element becomes more popular. Using the steel plates increases the lateral strength of the panel; meanwhile, it improves the ductility and energy dissipation capacity of the structure. This lateral force resistance system is approved by international codes such as IBC [1] and ASCE 7 [2].

In order to design and calculate the strength of CFS frames sheathed by thin steel plates, the North American Standard for Cold-Formed Steel Framing–Lateral Design (AISI S213-07 [3]) has been proposed tabulated nominal shear strength for some specific wall configurations based on a limited number of full-scale experimental results.

In last few years, some researchers were interested in investigating the performance of CFS shear walls. Therefore, a number of experimental programs were conducted by researchers for studying the seismic design parameters, evaluating the shear strength of panel and investigating the effects of different details on the performance of CFS steel shear walls.

One of the first experimental programs was carried out by Serrette [4] at Santa Clara University. In his study, some specimens with 2:1 and 4:1 aspect ratios were tested. The height of steel sheeting was 2.44 m and the widths were 1.22 m and 0.61 m. The thickness of frame members was 0.033 in (0.84 mm), and the thickness of steel sheeting were 0.018 in (0.46 mm) and 0.027 in (0.69 mm). The SPD (Sequential Phased Displacement) load protocol was used for performing cyclic tests. The results of his study were used in AISI S213-07 as nominal strength of CFS steel shear wall. In another research, which was conducted by Yu [5] at the University of North Texas, some of the Serrette tests was repeated using CUREE (Consortium of Universities for Research in Earthquake Engineering) loading protocol. The observed differences between the outcomes of Yu and Serrette tests for the 0.027 in (0.69 mm) thick steel sheet provided the basis for another research, which was conducted by Ellis [6]. Ellis also studied the effect of using CUREE and SPD loading protocols and the method of hold-downs installation.

Yu [7] conducted another research at the University of North Texas for verifying the values provided in AISI S213-07(AISI Lateral Design Standard 2007) [3]. This study was done for 0.018 in (0.46 mm) and 0.027 in (0.69 mm) thick sheeting and for investigating the behavior of shear walls with 4:3 aspect ratios. Nisreen Balh and Colin A Rogers [8] carried out an experimental program at McGill University with the purpose of developing Canadian seismic design provisions for steel-sheathed shear walls.

Shakibanasab et al. [9] studied the accuracy of the reduction factor of 2w/h for shear walls with height to width aspect ratio (h/w) > 2:1, which is stated in design provisions of CFS structures for satisfying allowable story drift limit, using the results of previous tests and new

* Corresponding author at: Noori Highway, P.O. Box 13145-1696, Tehran, Iran.
E-mail address: n.attari@bhrc.ac.ir (N.K.A. Attari).

http://dx.doi.org/10.1016/j.jcsr.2016.03.025
0143-974X/

Table 1
Specimen details.

Row	Specimen name	Wall dimension h × w (ft × ft) (mm × mm)	Nominal sheet thickness (in) & (mm)	Nominal frame thickness (in) & (mm)	Screw spacing at panel edges (in) & (mm)	Detail
1	2 × 8–33–27–2–S	8 × 2 (2440 × 610)	0.027 (0.69)	0.033 (0.84)	2 (50)	–
2	2 × 8–54–27–2–B	8 × 2 (2440 × 610)	0.027 (0.69)	0.054 (1.37)	2 (50)	Sheathing on two sides
3	4 × 8–33–27–2–S	8 × 4 (2440 × 1220)	0.027 (0.69)	0.033 (0.84)	2 (50)	–
4	4 × 8–33–27–2–B	8 × 4 (2440 × 1220)	0.027 (0.69)	0.033 (0.84)	2 (50)	Sheathing on two sides
5	4 × 8–43–27–2–S	8 × 4 (2440 × 1220)	0.027 (0.69)	0.043 (1.09)	2 (50)	–
6	4 × 8–54–27–2–B	8 × 4 (2440 × 1220)	0.027 (0.69)	0.054 (1.37)	2 (50)	Sheathing on two sides

1–No. 8 × 18–3/4–in. self–drilling truss Phil head screws were used for steel specimens.
2–Screw spacing was 12 in. in the field of sheathing for all specimens.
3–The studs were placed 24–in. from the edge, in the center.
4–Double back–to–back studs were used for the boundary, and single stud was used for the interior.
5–Nominal stud geometry (mm): web depth = 89, flange width=41, lip depth = 13.
6–Nominal track geometry (mm): web depth = 92, flange width = 38
7–Hold–Downs: Four Simpson Strong–Tie S/HTT14 hold–downs with 16–No. 10 × 1 in HWH self–drilling screws.

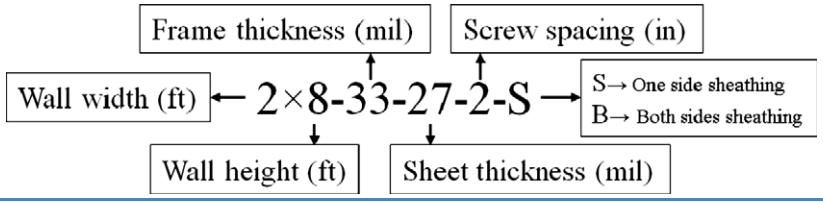

specimens that was test by them. The results of their investigation indicate that the reduction factor (2w/h) is conservative and a new equation for the reduction factor was proposed.

Another new research was conducted by Javaheri et al. [10], which involved 24 full-scale steel shear walls that tested under cyclic loading with different configurations of studs and screws. They studied the performance of CFS steel plate sheathed walls in terms of maximum lateral load capacity, load-deformation behavior, evaluating the failure modes of the panel and the factors that are contributing to the ductile response of specimens.

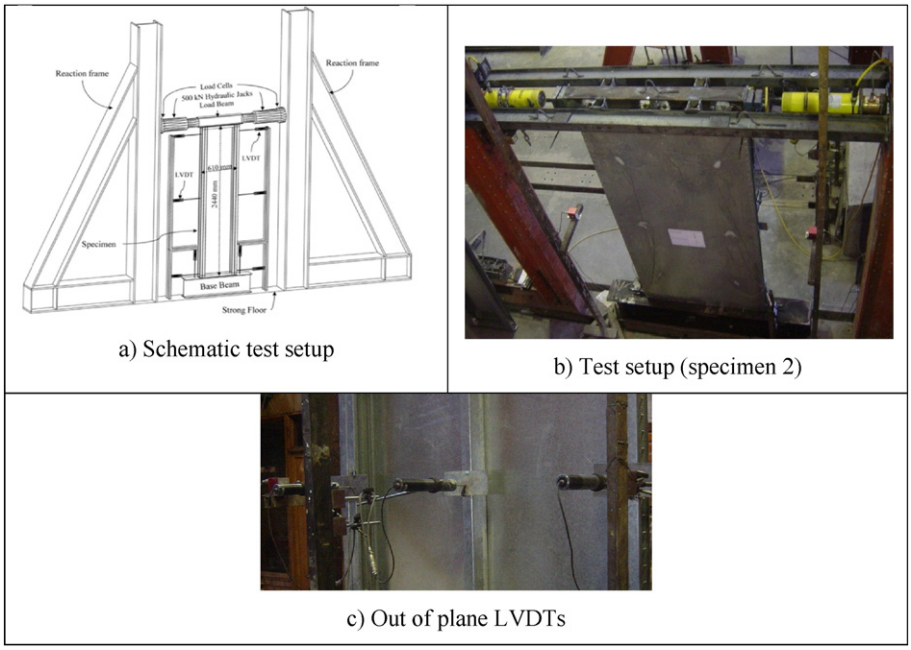

Fig. 1. Test setup.

Table 2
Material properties.

Sample	Thickness (mm)	Yield stress, F_y (MPa)	Tensile strength, F_u (MPa)	F_u/F_y
S1–27 mil steel sheet	0.7	265.0	292.8	1.10
S2–27 mil steel sheet	0.69	266.0	295.7	1.11
S3–27 mil steel sheet	0.69	264.0	290.4	1.10
T1–33 mil stud/track	0.84	293.3	338.8	1.16
T2–33 mil stud/track	0.83	293.7	338.1	1.15
T3–33 mil stud/track	0.83	301.3	341.4	1.13

Mohebbi et al. [11] conducted an Experimental investigation on cold-formed steel (CFS) shear walls consisted of one and two side steel-sheathed specimens. In this study, six CFS wall specimens were tested under reversed cyclic loading. Different frame and steel sheeting thicknesses were used in the construction of these samples. The parameters that were investigated in this research program include failure modes, energy dissipation capacity, shear strength and elastic stiffness.

Yu and Chen [12] studied the performance of 1.83 m wide, 2.44 m high cold-formed steel stud framed shear walls using one-sided steel sheet sheeting. They proposed a special detailing to prevent the failure in the studs. Furthermore, in their research, the nominal shear strength of 1.83 m wide one-sided CFS shear walls was established for design purposes. Another newly conducted investigation is done by Wang and Ye [13]. Their study was consisted of investigating the performance of cold-formed steel shear walls with concrete-filled rectangular steel tube columns as end studs to prevent collapsing due to compression buckling of the end studs. The studied parameters were consisted of the influence of stud type, sheeting material and openings. On the other hand, using two-sided CFS shear walls with other materials is becoming more popular such that a number of researches are concentrated on this subject. Zeynalian and Ronagh [14] focused their experimental research on both two-sided and one-sided fiber-cement boards (FCB) shear panels.

According to the literature, almost all of the tests were done on one side sheathed CFS steel plate shear walls, also the North American Standard for Cold-Formed Steel Framing–Lateral Design (AISI S213) has been proposed tabulated nominal shear strength for one side sheathed CFS frames with some specific wall configurations. However, for two-sided CFS steel plate shear walls, it is mentioned in this code that for walls with the same material and nominal strength, applied to opposite side of the frame, the total available strength is cumulative. In this study, six one and two-sided steel-sheathed CFS frames are tested under reversed cyclic loading to investigate the nominal shear strength and to compare this strength with the AISI S213 statement. Furthermore, the seismic performance and the local buckling pattern of two-sided steel-sheathed specimens are studied. For further investigation, test specimens are simulated numerically using ABAQUS [15] software and verified with test results. In addition, twelve extra numerical models are created to study the effects of various steel plates and frame thicknesses on the capacity of CFS steel shear walls.

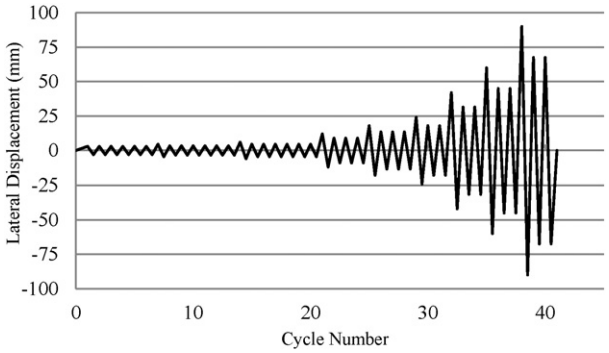

Fig. 2. Loading pattern.

2. Test program

The experimental program consists of six CFS shear walls sheathed with thin steel plates. The tests were carried out at Building and Housing Research Center (BHRC) laboratory.

The main aim of this research is to investigate the performance of the shear wall panels with the steel plate sheathed on two sides, therefore three specimens are two-sided and the others are one-sided walls. All of the specimens are designed based on Table C2.1–3 of AISI S213-07, which presents the nominal shear strength of shear wall based on the minimum thicknesses of track and stud elements, minimum sheeting screw size and fastener spaces at panel edges. In this code, the nominal strength of the shear wall is presented based on the Serrette [4] tests, which considered failure mode in them is steel sheeting rupture and other failure modes are neglected. In this paper, the effects of other failure modes in walls' lateral strength are investigated.

The specimens are tested under lateral loading without consideration of gravity loads. Imposing the gravity loads lead to decrease the lateral strength and the ductility of walls. It should be mentioned that in CFS structural design, walls with steel sheathed are placed in a manner that they have no or very small gravity loads. This procedure is used because the cold-formed sections are usually sensitive to compression loads, and using them as boundary element of shear walls applies a large compression demand on these sections. Therefore imposing gravity loads lead to decrease in lateral load resistance capacity of shear walls and it is better to be avoided.

2.1. Specimen details

In this study, six specimens consist of four 2:1 and two 4:1 aspect ratio shear wall panels are investigated. The specimens include 2.44 m height, 1.22 m and 0.61 m widths. The thicknesses of frame members are 0.033″ (0.84 mm), 0.043″ (1.09 mm) and 0.054″ (1.37 mm) and the thickness of steel sheeting are 0.027″ (0.69 mm). Table 1 listed in detail the specification of each specimen such as screw fastener schedule, dimensions of studs and tracks, and hold down devices.

2.2. Test setup

The test setup is shown in Fig. 1. A load beam is connected to the top of the wall to impose the lateral forces. Four 1.2 in.-diameter bolts are used to fix the load beam to the top track. The bottom of the specimens is attached to a plate girder for facilitating the connection of the wall to the laboratory strong floor. The Lateral support beams braced laterally to prevent out of plane movements during the tests. Two 500-kN hydraulic jacks are located on each side of the top of the wall for imposing the lateral loads. Two load cells placed between hydraulic jacks and loading frame for recording the lateral forces. Two LVDTs (Linear Variable Differential Transformers) utilized at the top level of the wall to measure the displacements during the tests. Two other LVDTs attached to the mid height of the wall, and seven others at various points of the wall for recording uplift of the wall, slippage and out of plane buckling of stud (Fig. 1c).

Fig. 3. Specimen 1 (2 × 8-33-27-2-S) Lateral load-displacement response and buckling pattern.

2.3. Material properties

Three coupons were randomly selected from the steel sheeting and three coupons were extracted from the flanges and webs of frame members. Tensile tests have been done on these samples according to ASTM A370-06 [16]. The results of tensile tests are listed in Table 2. Based on ASTM A1003 [17] the grade of the steel materials in the frame and sheeting are ST230H.

2.4. Loading protocol

Reversed cyclic loading protocol in accordance with method C of ASTM E2126 (2007) [18] is employed for determining the shear strength of the walls. Fig. 2 shows the loading protocol of the testing program. The amplitude of reference displacement (Δ) was selected equal to the 2.5% of story height, which is the maximum allowable drift for conventional structures with the CFS frame system according to ASCE 7–10 [2].

3. Test results

The specimens are investigated in terms of local buckling patterns, failure modes and lateral load-story displacement hysteretic response. The height to width aspect ratio (h/w) of first and second specimens are 4:1. As it is listed in Table 1, specimen 2 is two-sided wall, and the frame thickness of specimen 1 and 2 are 0.84 mm and 1.37 mm respectively. The height to width aspect ratio (h/w) of specimens 3 to 6 are 2:1. Walls 3 and 4 are identical in terms of frame and steel panel thickness and screw schedule, while the specimen 4 is two sides

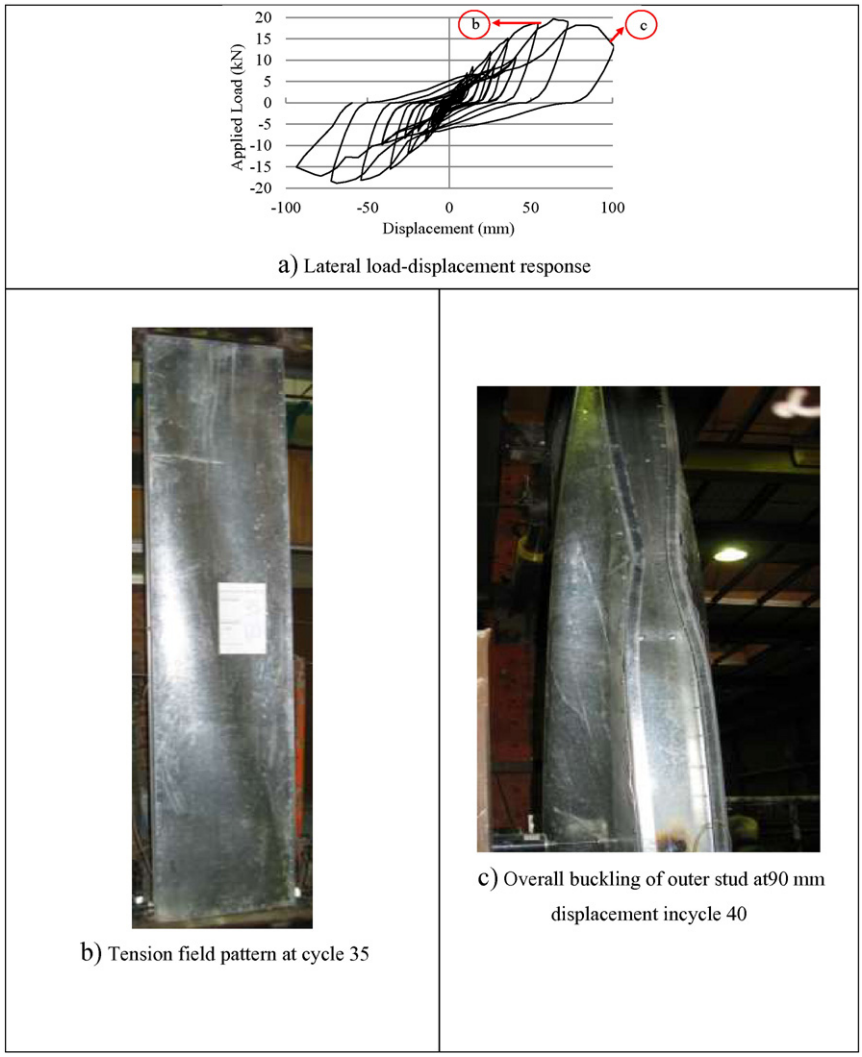

Fig. 4. Specimen 2 (2 × 8-54-27-2-B) Lateral load-displacement response and buckling pattern.

sheathed. Samples 5 and 6 are the same as specimens 3 and 4 with different frame member thickness.

3.1. Specimen 1 (2 × 8-33-27-2-S)

Fig. 3a shows the lateral load-story displacement response of specimen 1, which is consisted of 0.69 mm one-side steel sheeting, and 0.84 mm framing. In this wall (2 × 8-33-27-2-S) the tension field pattern along the diagonal of the wall occurred at 24 mm lateral displacement (Fig. 3b). Buckling of steel sheeting between screws is the dominated failure mode of this specimen that started at the 37 mm lateral displacement. With increasing the lateral displacement up to 42 mm in this cycle, wrinkling of steel sheeting caused local buckling in the stiffener of outer stud flange of boundary element at the middle height of the wall as shown in Fig. 3c and d. In the outer flange of boundary element at the middle height of the wall, torsional buckling occurred and then caused to overall buckling in middle height of the specimen. The ultimate capacity of this wall is about 9.8 kN, which is equal to 16.05 kN/m in wall's width. Overall buckling of specimen caused to decline the lateral strength by nearly 50% of ultimate strength. The locations of different failure modes during loading are shown on the hysteresis curve (Fig. 3a). The mentioned failure mode, which happened in this specimen, is not considered in the proposed capacity for CFS shear walls sheathed with the steel plate in AISI S213–07.

3.2. Specimen 2 (2 × 8-54-27-2-B)

Specimen 2 × 8-54-27-2-B, which is consisted of 0.69 mm two-side steel sheeting, and 1.37 mm framing shows the best performance among other walls in terms of sustaining lateral load at higher drift levels. The sample did not lose strength after 40 cycles (90 mm lateral displacement). Fig. 4a shows the lateral load-story displacement response of specimen 2.

In this specimen, the tension field pattern along the diagonal of wall occurred in both sheeting at 50 mm lateral displacement (Fig. 4b). The first failure mode was local buckling of boundary element, which began in cycle 40 (85 mm lateral displacement). After that, overall buckling of specimen happened at 90 mm lateral displacement (Fig. 4c).

The ultimate capacity of this wall is about 19.3 kN, which is equal to 31.64 kN/m in wall's width. As can be seen, overall buckling caused to decrease the lateral strength of the wall by nearly 30% at 90 mm displacement.

3.3. Specimen 3 (4 × 8-33-27-2-S)

Fig. 5 shows the Lateral load-displacement response and buckling patterns of specimen 3, which is consisted of 0.69 mm one-side steel sheeting, and 0.84 mm framing. In this wall (4 × 8-33-27-2-S) the tension field pattern along the diagonal of the wall occurred at 12 mm

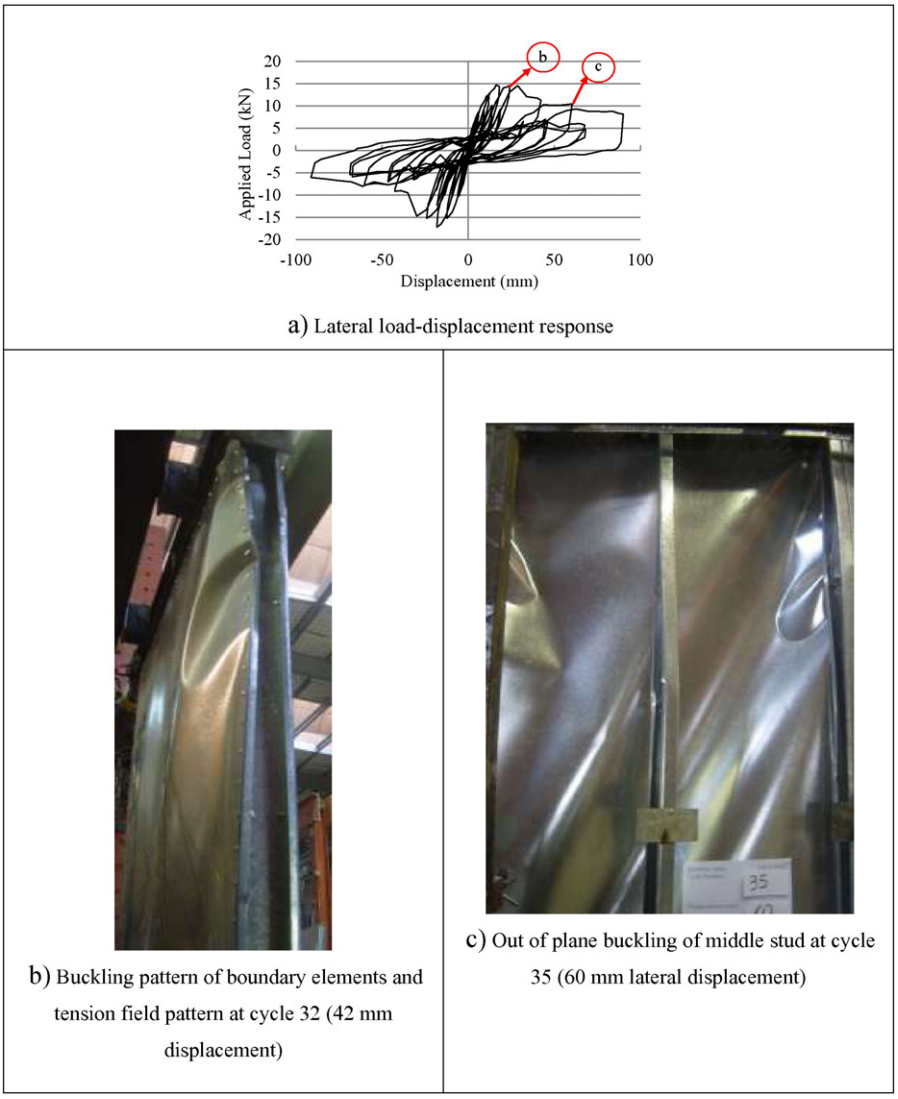

Fig. 5. Specimen 3 (4 × 8-33-27-2-S) Lateral load-displacement response and buckling pattern.

lateral displacement. The first failure mode started at cycle 25 (18 mm displacement) which was the buckling of the outer stud flange of boundary element caused by tensile field pattern of steel sheeting at upper corners of the wall. Damage of the specimen continued with screws pull out in the middle of stud caused by severe buckling in steel sheeting due to diagonal tension field. At cycle 32 (42 mm displacement), boundary elements buckled in the upper corner of the wall. With increasing the lateral displacement, boundary elements buckled completely and the middle stud of the wall buckled in out of plane direction and complete failure of wall happened at cycle 35 (60 mm lateral displacement). The ultimate capacity of this wall is about 17.2 kN, which is equal to 14.11 kN/m in wall's width. Overall buckling of specimen significantly reduced the lateral strength of specimen by nearly 50% of ultimate strength.

3.4. Specimen 4 (4 × 8-33-27-2-B)

Fig. 6a shows the lateral load-story displacement response of specimen 4, which is consisted of 0.69 mm two-sides steel sheeting, and 0.84 mm framing. In this wall (4 × 8-33-27-2-B) the tension field pattern along the diagonal of the wall occurred at 10 mm lateral displacement. The main failure pattern in this specimen was buckling of the boundary studs above the hold-down fasteners at the corner of the wall. This failure mode began at cycle 25 (18 mm lateral displacement). Increasing the displacement leads to plastic hinges formation in boundary elements at 500 mm above the lower track and decrease in the shear capacity. With increasing the lateral displacement, wall rotated around the plastic hinge and caused the stud rupture at 90 mm displacement (Fig. 6c). The ultimate capacity of this wall is about 22.92 kN, which is equal to 18.79 kN/m in wall's width. Buckling of the boundary studs caused to decline significantly the lateral strength by nearly 30% of ultimate strength.

In this specimen since the ratio of sheeting strength to the boundary studs strength is high, buckling of boundary elements governs the performance of this wall. As can be seen, in Fig. 6a, the strength of the wall experience a fast decline at 18 mm lateral displacement because of boundary element buckling which is the most brittle failure mode of shear walls sheathed with the steel plate in CFS structures.

As mentioned before this specimen was designed according to AISI S213.·Based on the test results, it seems that the minimum studs' thickness expressed in the AISI S213 should be increased, or studs should be designed for the lateral capacity of walls.

3.5. Specimen 5 (4 × 8-43-27-2-S)

Fig. 7a shows the lateral load-story displacement response of specimen 5, which is consist of 0.69 mm one-side steel sheeting, and 1.09 mm framing. In this wall (4 × 8-4327-2-S) the tension field pattern

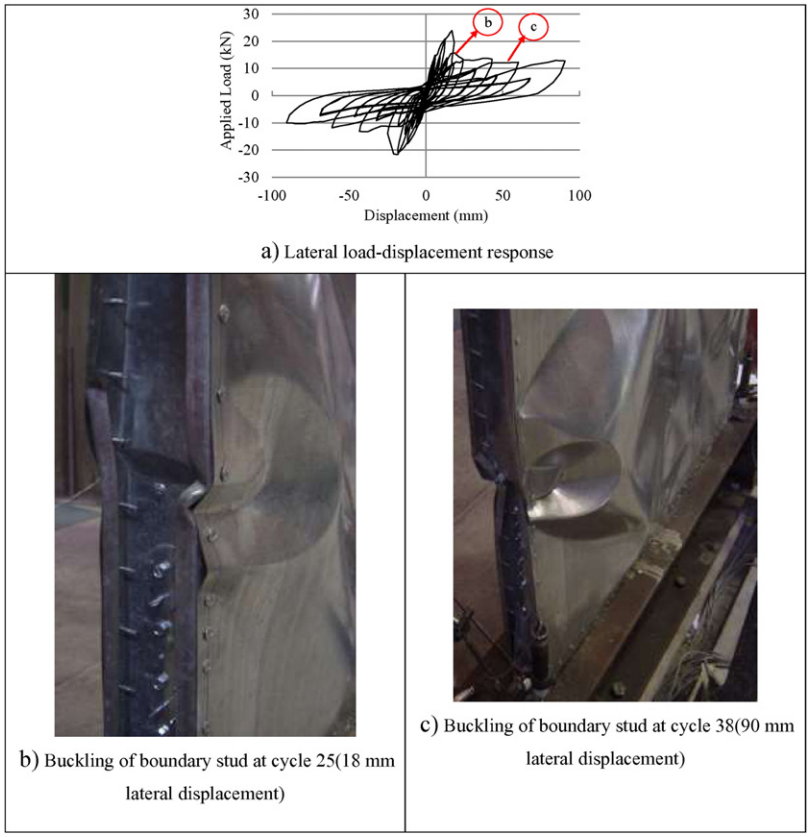

Fig. 6. Specimen 4 (4 × 8-33-27-2-B) Lateral load-displacement response and buckling pattern.

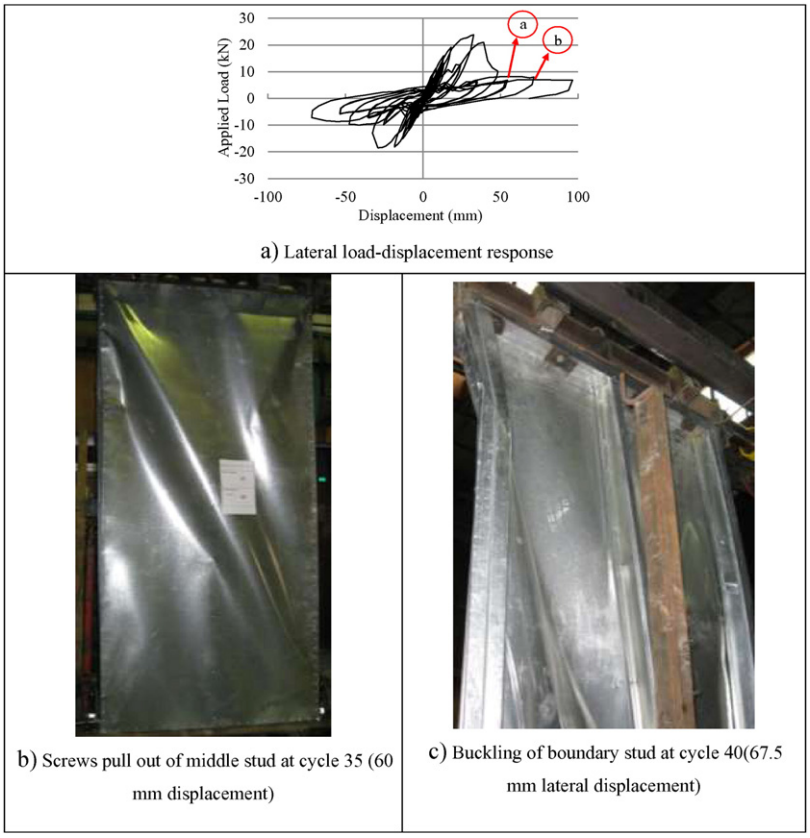

Fig. 7. Specimen 5 (4 × 8-43-27-2-S) Lateral load-displacement response and buckling pattern.

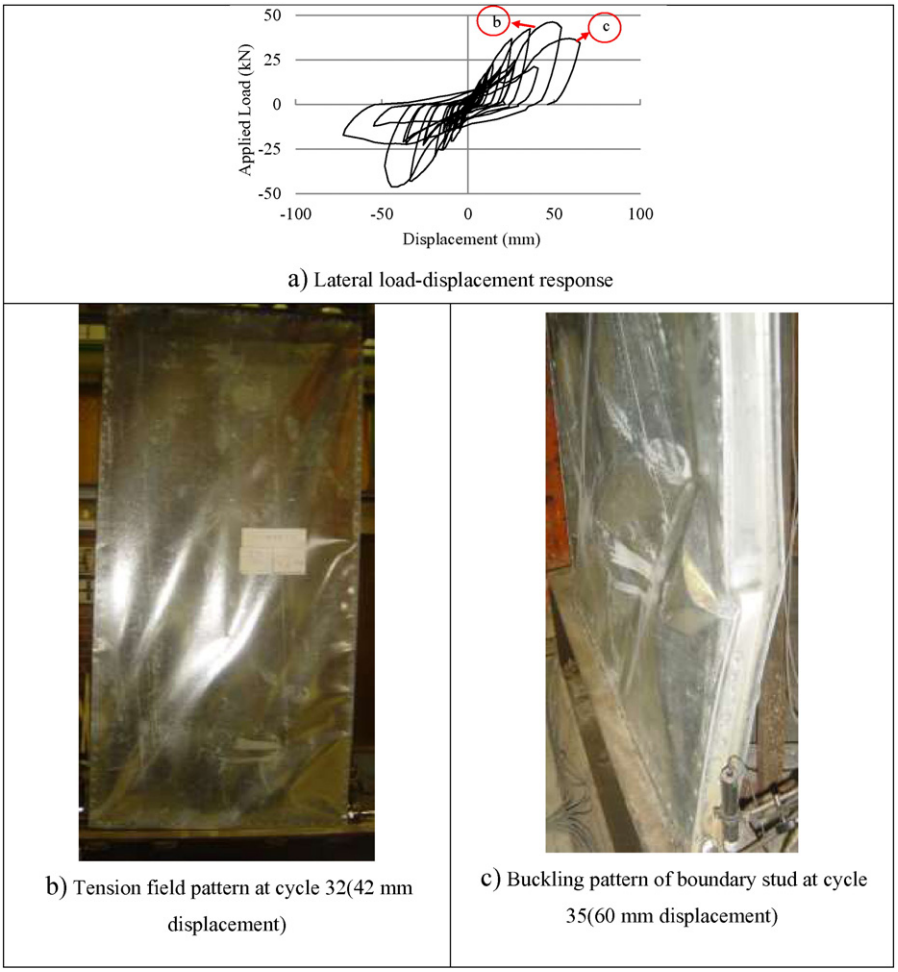

Fig. 8. Specimen 6 (4 × 8-54-27-2-B) Lateral load-displacement response and buckling pattern.

along the diagonal of the wall occurred at 15 mm lateral displacement. Specimen 5 experienced no specific failure up to cycle 30(24 mm displacement). The first buckling started at cycle 32 (42 mm displacement), which was the distortion of outer flange of boundary elements due to tension field pattern of steel sheeting at the upper corner of the wall. At cycle 35(60 mm displacement), screws pull out of middle stud occurred due to severe wrinkling of steel sheeting in diagonal tension filed (Fig. 7b).

With increasing the lateral displacement up to 67.5 mm lateral displacement in cycle 40, the boundary elements completely buckled (Fig. 7c). In this cycle, out of plane buckling of middle stud happened and caused a severe damage to the wall. The ultimate capacity of this wall is about 23.51 kN, which is equal to 19.28 kN/m in wall's width. Out of plane buckling of middle stud reduced the wall lateral strength up to 50% of ultimate strength (Fig. 7a).

3.6. Specimen 6 (4 × 8-54-27-2-B)

Fig. 8a shows the lateral load-story displacement response of specimen 6, which is consist of 0.69 mm two-side steel sheeting, and

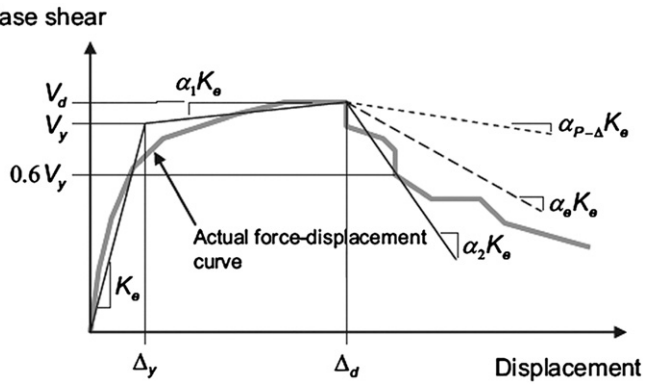

Fig. 9. Method used to develop idealized curve according to ASCE 41-13 [19].

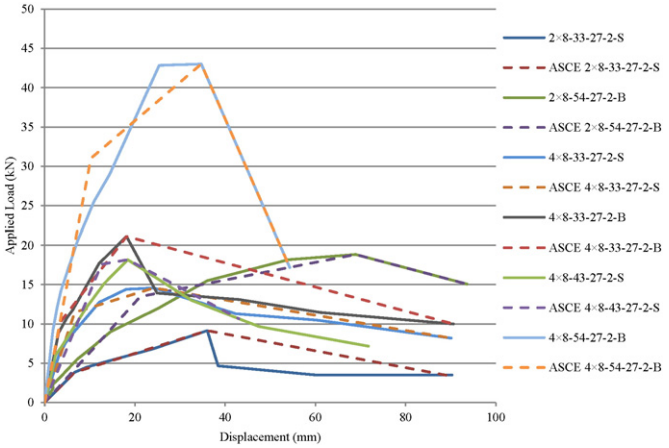

Fig. 10. Idealized curves according to ASCE 41-13.

Table 3
Structural properties for each specimen based on tests data.

Row	Specimen name	Effective stiffness (K_e) (kN-mm)	Maximum strength (V_d) (kN)	Yield strength (V_y) (kN)
1	2 × 8-33-27-2-S	0.58	9.16	3.83
2	2 × 8-54-27-2-B	0.63	18.83	13.47
3	4 × 8-33-27-2-S	1.72	14.57	11.46
4	4 × 8-33-27-2-B	2.55	17.19	10.48
5	4 × 8-43-27-2-S	1.39	18.17	17.58
6	4 × 8-54-27-2-B	3.03	43.01	31.01

1.37 mm framing. In this wall (4 × 8-54-27-2-B) the tension field pattern along the diagonal of the wall occurred at 18 mm lateral displacement. The overall behavior of specimen 6 is very similar to specimen 4. The first failure mode, which caused to decrease the lateral strength of the wall, started with buckling of steel sheeting in diagonal tension field and wrinkling of the plate between screws at corner areas of the specimen (Fig. 8b).

The main failure pattern in specimen 6 was the buckling of boundary studs above the hold-down fasteners at the corner of the wall, which happened at cycle 35 (60 mm displacement). Increasing the displacement led to global buckling in boundary elements above the hold-down fasteners, which decreased the shear capacity of the wall (Fig. 8c). Using thicker studs in this specimen compared to specimen 4 shifted the buckling of boundary elements to higher lateral displacement. The ultimate capacity of this wall is about 46.21 kN, which is equal to 37.90 kN/m in wall's width. Global buckling in boundary elements above the hold-down fasteners caused to decline the lateral strength about 50% of ultimate strength.

4. Structural characteristics of tested specimens

One of the lateral load resistance systems in CFS structures is steel-sheathed wall panels. Therefore, the structural performance of this system such as system overstrength and response modification factor is directly related to the performance of steel-sheathed walls.

To calculate the structural properties such as ductility, system overstrength and response modification factors, it is necessary to fit idealized force-displacement curve to each backbone curve of load-displacement. In this research, the method described in ASCE 41-13 [19] is used for this purpose (Fig. 9). In cases which the base shear does not degrade to 60% of the effective yield strength at the end of the test, the last point of the backbone carve is chosen as the end of the third line segment. The idealized curve for each specimen is shown in Fig. 10; also, the basic structural values for each specimen are shown in Table 3.

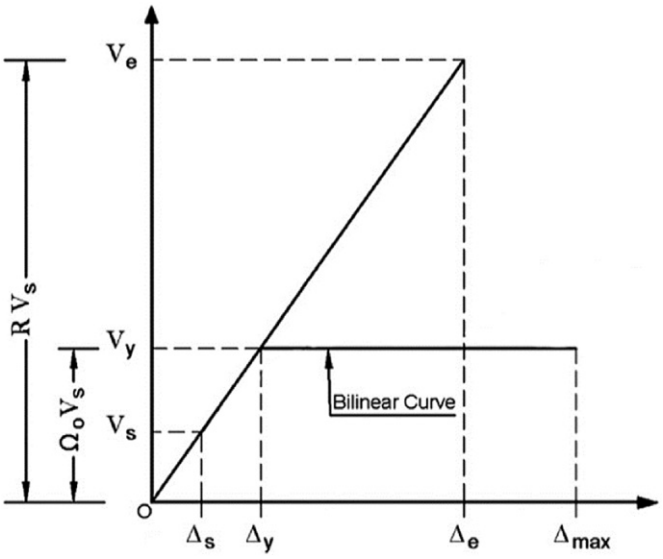

Fig. 11. Skeleton used to calculate structural properties:

In addition, response modification coefficient (R) is evaluated from experimental results. The R coefficient is described as a product of two factors. Based on Fig. 11 and using Eq. (1), the R coefficient can be calculated.

$$R = \frac{\Delta_e}{\Delta_s} = \frac{\Delta_e}{\Delta_y} \times \frac{\Delta_y}{\Delta_s} = R_\mu \Omega_0 \quad (1)$$

where R_μ is a period dependent ductility factor, Ω_0 is an overstrength factor, V_s is the base shear corresponding to the first yield of the structural elements that causes softening in the real backbone curve of the system, Δ_e is the displacement corresponding to ultimate elastic base shear. Δ_{max} is the maximum displacement, which is considered the displacement corresponding to the reduction of force to 80% of the maximum base shear strength and the rest of the parameters are as defined in Fig. 11.

To estimate the first yield point of the specimens, the data of hysteresis curves were monitored. Where the stiffness value started to decrease, it was assumed that the first yielding occurred. The ductility factor R_μ is used as a measure of the global nonlinear response of a framing system and it depends mainly on the ductility ratio μ and period T. According to the relation proposed by Newmark and Hall [20], R_μ is equal to $\sqrt{2\mu - 1}$ for $T < 0.5$ s and to μ for $T \geq 0.5$ s. The components of R are presented in Table 4.

As can be seen from Table 4, ductility, overstrength factor and response modification factor of this type of shear wall, highly depends on wall details and the ratio of boundary elements' strength to steel sheeting strength.

The overstrength factors (Ω_0) of the specimens are evaluated between 1 and 3.35 for specimens 1 and 6 respectively with the average of 2.08. The last column in Table 4 represents the R coefficient values that are computed from multiplying Ω_0 by the minimum of $\{R_\mu, \mu\}$. The values indicate that an average R coefficient for CFS shear wall sheathed by thin steel plates strongly depend on the wall details. The R coefficient of specimens varies between 3.31 and 7.24 with the average of 5.3. It should be noted that these tests were performed without imposing gravity loads, which can reduce the ductility of wall.

The variation in evaluated R coefficients is mainly because of the differences between the strength ratio of boundary elements and steel sheeting. This difference in the strength causes the specimens to perform in different manners and varying buckling modes govern the ultimate strength of the specimens. In this study, the term of “weak boundary element” denotes the specimens in which the boundary element buckling governs the wall's performance and on the contrary, “strong boundary element” denotes the specimens that the boundary elements are able to sustain axial forces without severe buckling.

Nisreen Balh and Colin A. Rogers [8] have been evaluated the ductility related force modification factor (R_μ) for their tested specimens. In their research, Equivalent Energy Elastic Plastic (EEEP) was used for simplifying the test results to bilinear elastic-plastic curve. The obtained average value for reversed cyclic tests in their research is 2.81, which is very close to average evaluated in present paper that is 2.77.

Table 4
Evaluated response modification factors.

Specimen name	Overstrength factor Ω_0			Ductility ($\mu = \Delta_{max}/\Delta_y$)			Ductility factor (R_μ)($T < 0.5$ s)			Response modification coefficient (R)		
	Positive backbone	Negative backbone	Average	Positive backbone	Negative backbone	Average	Positive backbone	Negative backbone	Average	Positive backbone	Negative backbone	Average
2 × 8-33-27-2-S	1	1	1	6.39	5.61	6	3.43	3.2	3.315	3.43	3.2	3.315
2 × 8-54-27-2-B	2.19	1.95	2.07	3.74	4.42	4.08	2.55	2.8	2.675	5.58	5.46	5.52
4 × 8-33-27-2-S	1.91	1.33	1.62	3.49	7.07	5.28	2.45	3.62	3.035	4.68	4.81	4.745
4 × 8-33-27-2-B	1.35	1.19	1.27	5.27	6.24	5.755	3.09	3.39	3.24	4.17	4.03	4.1
4 × 8-43-27-2-S	3.4	3.31	3.355	2.98	2.25	2.615	2.23	1.87	2.05	7.58	6.19	6.885
4 × 8-54-27-2-B	3.55	2.79	3.17	2.5	4.01	3.255	2	2.65	2.325	7.1	7.39	7.245

ASCE7–10 specifies that the value of Ω_0 of CFS structures with steel shear wall should be taken as 2.5 and it specifies that the R factor should be considered as 7 for this type of structure.

Although these tests are not adequate for concluding about structural characteristics, but the results revealed that if the capacity of brittle failure modes governs the performance of the shear wall, the ductility and system overstrength factor will be lower than the ASCE7–10 values and it should be considered in design procedure.

5. FEM modeling verification

The finite element method (FEM) is one of the most widely accepted numerical solutions for exploring engineering problems. Therefore, in this study, nonlinear FEM is employed for more investigation on the overall performance and buckling patterns of CFS shear wall. ABAQUS software, which is one of the most commonly, used FEM tools, is utilized in this research for simulating the models.

At the first step, the specimen 2 × 8-33-27-2-S is used for verification of FEM models. Then, twelve further models are investigated using the assumptions of the verified model.

5.1. Model specification

The different parts of the simulated models are illustrated in Fig. 12. As it is shown, all parts of the model, including studs, tracks and steel sheeting are simulated using four node shell elements that are known as S4R elements in the ABAQUS software. Based on a short parametric study on the mesh size, the 10 mm mesh size was found adequate for modeling the track, stud and steel sheeting. The specimens' details, boundary conditions and materials are accurately modeled based on the tests details. Fig. 13 presents the boundary conditions and loading regions used for numerical models. As it is shown in Fig. 13, the lateral load is applied to the top track of the model (red regions) at the same regions where the loading beam was attached to the tested specimens. On the other hand, the simulated models are restrained at the bottom track at the regions where the hold down ties were used in experiments (red regions in Fig. 13).

The connections between the frame and the steel sheeting are modeled via fastening the frame and the steel sheet at the screw points using Cartesian Connector existing in ABAQUS [15] software library. The characteristics of the fasteners are modeled using elastic behavior of the screws. In this study, based on the experimental observations, the screw pull out behavior is not considered in models. The contact between steel sheeting and studs or tracks is simulated using "surface to surface contact" such that separation is allowed during the analysis.

5.2. Material models and material properties

The nonlinear behavior of the frame and the steel sheeting were simulated using an isotropic hardening model based on the von Mises yield criterion. This material model is known as "Classical metal plasticity" in ABAQUS [15] software library. The material characteristics were defined according to the result of uniaxial tension tests, which are listed in Table 2.

5.3. Model verification

In order to verify the results of the numerical model with the experimental study, specimen 1 is simulated. Due to high computational costs, simulation of two-sided steel sheeting specimens or specimens with height to width aspect ratio (h/w) 2:1 was practically impossible.

The authors tried to simulate the specimen 4 × 8-43-27-2-S but the analysis stopped at 32 mm lateral displacement due to running out of memory space. The numerical result of this specimen is presented in

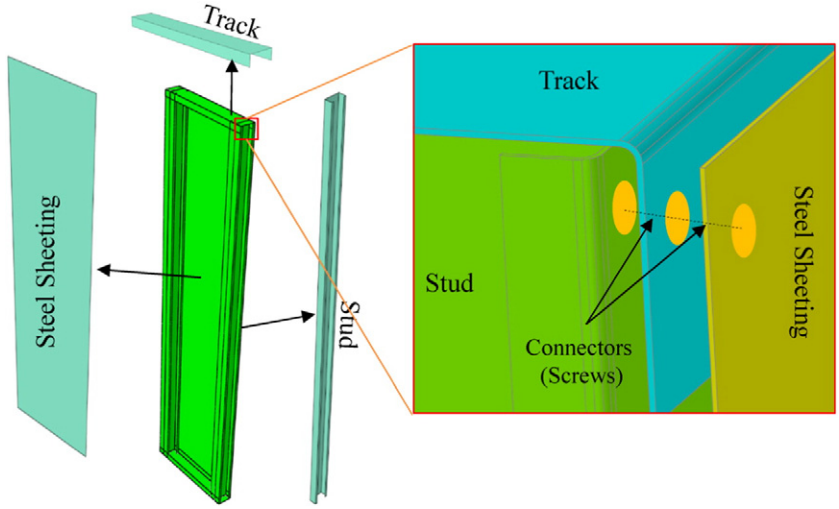

Fig. 12. Simulated model.

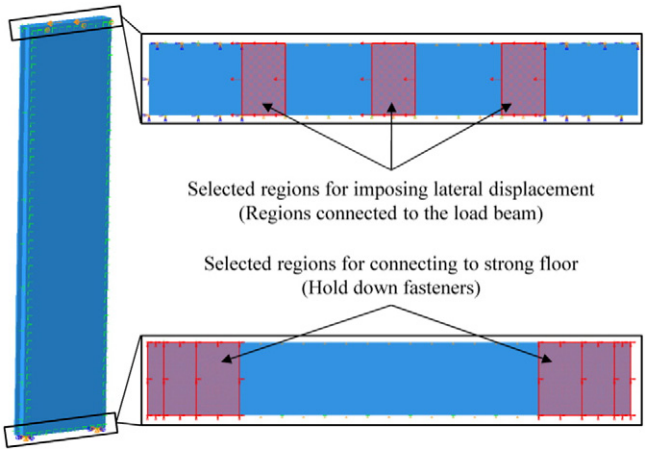

Fig. 13. Boundary conditions of simulated model.

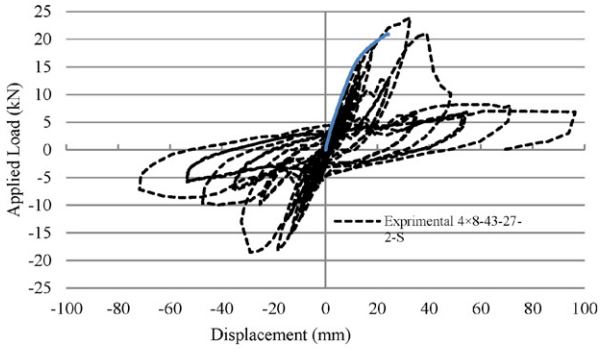

a) Lateral load-displacement response

b) Tension field pattern of tested wall

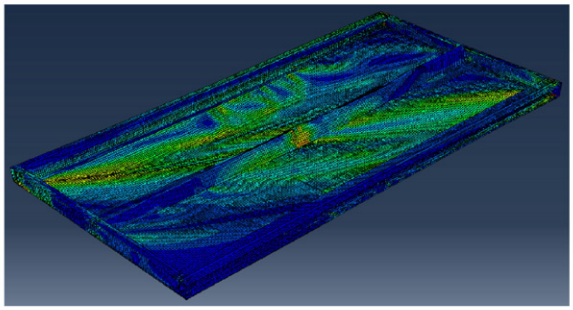

c) Tension field pattern of FEM model

Fig. 14. Lateral load-story displacement response and buckling pattern of numerical simulation of specimen 2 × 8-33-27-2-S.

Fig. 14. As it is shown in this figure, the analysis stopped at 32 mm displacement.

The parameters that are considered for verification are as the following: lateral load-story displacement response and local buckling patterns of boundary elements and steel sheeting.

5.3.1. Lateral load-story displacement response

Fig. 15 presents the lateral load-story displacement response of the tested wall and FEM analysis results. As it is shown in this figure, the numerical results indicate very good agreement with test results in terms of initial stiffness, the peak strength estimation and post buckling response. The initial stiffness of the test and numerical model are 0.767 kN/mm and 0.876 kN/mm, respectively, which represents 14% difference between experimental results and FEM. The ultimate strengths of test and simulated model are 9.83 kN and 10.56 kN respectively, which is equal to 7.5% variance. A little difference between the finite element model and the experimental results is due to several parameters such as lack of simulating the screw pull out phenomenon, imperfections of tested specimens and different material properties, which the numerical model was unable to capture them.

5.3.2. Buckling patterns

As it maintained before, the main failure mechanism of tested models were studs and steel sheeting buckling. Therefore, the models are simulated considering the nonlinear geometry to capture the buckling patterns of elements. Fig. 16 shows the buckling patterns of tested specimens and simulated models. It can be concluded from this figure that the models are successful in capturing the tension field in the steel sheeting and studs buckling patterns. It should be noted that for imposing an imperfection to the simulated models, the middle point of the steel sheeting is pushed 10 mm out of plane, prior to lateral pushover analysis. Imposing the imperfection helps to attain results that are more realistic.

6. Case study

In this research, twelve further numerical models are investigated using verified FE model. The aim is to study the effects of different wall and sheeting thicknesses. The responses of the numerical models are investigated in terms of Lateral Load-Story Displacement Response and Buckling Patterns. It should be mentioned that in these models, screw pull out is not simulated (a full explanation is presented in Section 5.1).

All of these numerical models are similar to specimen 1 in terms of configuration, height to width aspect ratio (h/w) and are sheathed on one side. Details of all simulated models are presented in the Table 5. The naming pattern of all models is the same as in Table 2.

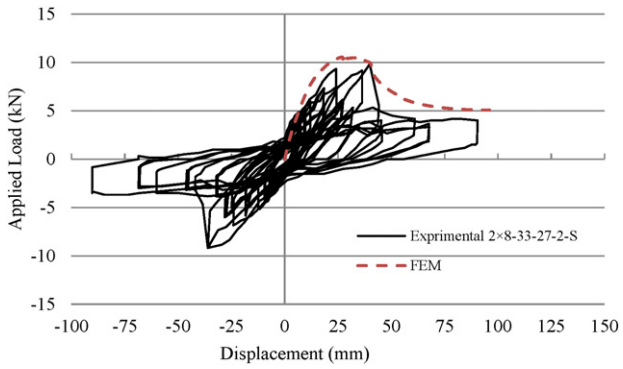

Fig. 15. Lateral load-story displacement response of numerical simulation and tested specimen 2 × 8-33-27-2-S.

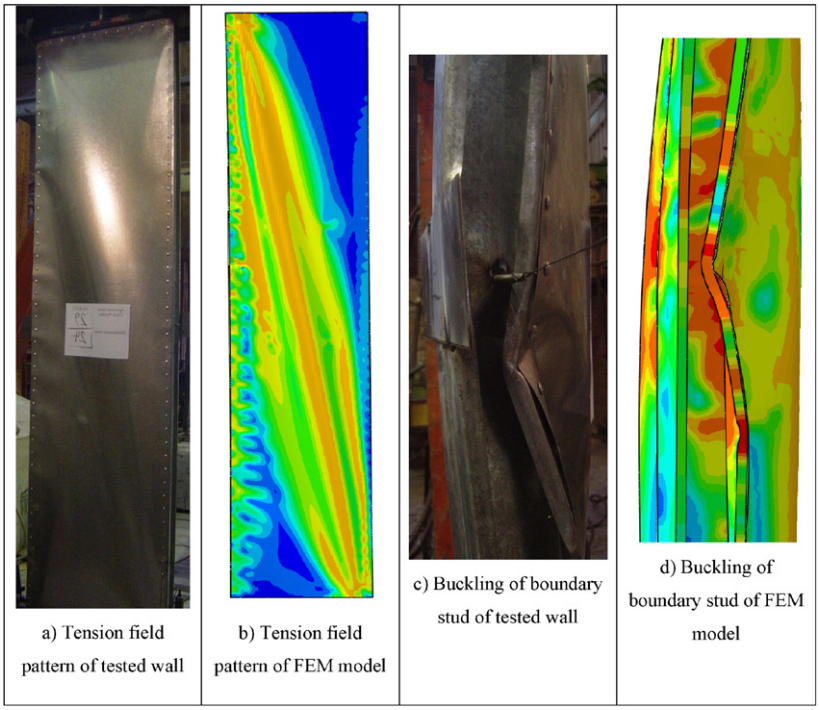

Fig. 16. Buckling pattern of tested specimen and FEM model.

6.1. Lateral load-story displacement response

Fig. 17 shows the lateral load-story displacement of numerical models in four groups. Each group represents the result of the pushover analysis of the walls with the same sheeting thickness and various frame thicknesses. The analysis of some models such as M5, M9, M10 and M12 have not been completed due to numerical convergence difficulties, therefore lateral load-story displacement curves are presented up to end point of analysis. Based on Fig. 17 it can be seen that increasing the frame thickness can influence the performance of the walls in terms of ultimate strength, initial stiffness and failure modes.

In CFS shear walls sheathed with steel plate, the boundary studs are under high axial loads caused by lateral force. Therefore, the capacity of the shear wall has a correlation with the ultimate strength of these elements. Using studs with low thickness compared with steel sheeting causes to decrease initial stiffness as well as the ultimate strength of shear wall and may lead to brittle failure of shear wall. To find out the influence of different frame thicknesses, the ratio of ultimate strength of simulated models to frame thickness vs. steel sheeting thickness is depicted in Fig. 18. As can be seen, there is a linear relation between the steel sheeting thickness and the ratio of ultimate strength to frame thickness.

In models with low frame thickness, buckling of boundary studs govern the behavior of the wall, while in models with higher frame thickness failure mode is controlled with steel sheeting yielding. Therefore, the influence of stud's axial capacity in ultimate strength becomes smaller with increasing the frame thickness.

Furthermore, the stiffness of models is calculated using secant stiffness at a lateral force equal to 40% of the ultimate strength of each model. The secant stiffness and ultimate strength of all models are presented in Table 6. The secant stiffness of models M1, M5, M8 and M11 are 0.784, 0.966, 1.169 and 1.282 kN·mm, which shows the stiffness of specimens rise with increasing in the nominal steel sheeting thickness. On the other hand, this table shows the walls stiffness increase with increasing the frame thickness too.

The most remarkable difference between the responses of models is the post peak behavior of them. The post peak negative slope of models highly depends on the ratio of nominal frame thickness to steel sheeting

Table 5
FE model details.

Row	Model name	Wall dimension h × w (ft × ft) (mm × mm)	Nominal sheet thickness (in) & (mm)	Nominal frame thickness (in) & (mm)	Screw spacing at panel edges (in) & (mm)
M1	2 × 8-33-27-2-S	8 × 2 (2440 × 610)	0.027 (0.69)	0.033 (0.84)	2 (50)
M2	2 × 8-43-27-2-S	8 × 2 (2440 × 610)	0.027 (0.69)	0.043 (1.09)	2 (50)
M3	2 × 8-54-27-2-S	8 × 2 (2440 × 610)	0.027 (0.69)	0.054 (1.37)	2 (50)
M4	2 × 8-27-33-2-S	8 × 2 (2440 × 610)	0.033 (0.84)	0.027 (0.69)	2 (50)
M5	2 × 8-33-33-2-S	8 × 2 (2440 × 610)	0.033 (0.84)	0.033 (0.84)	2 (50)
M6	2 × 8-43–33-2-S	8 × 2 (2440 × 610)	0.033 (0.84)	0.043 (1.09)	2 (50)
M7	2 × 8-54-33-2-S	8 × 2 (2440 × 610)	0.033 (0.84)	0.054 (1.37)	2 (50)
M8	2 × 8-33-43-2-S	8 × 2 (2440 × 610)	0.043 (1.09)	0.033 (0.84)	2 (50)
M9	2 × 8-43-43-2-S	8 × 2 (2440 × 610)	0.043 (1.09)	0.043 (0.84)	2 (50)
M10	2 × 8-54-43-2-S	8 × 2 (2440 × 610)	0.043 (1.09)	0.054 (1.37)	2 (50)
M11	2 × 8-33-54-2-S	8 × 2 (2440 × 610)	0.054 (1.37)	0.033 (0.84)	2 (50)
M12	2 × 8-43-54-2-S	8 × 2 (2440 × 610)	0.054 (1.37)	0.043 (1.09)	2 (50)
M13	2 × 8-54-54-2-S	8 × 2 (2440 × 610)	0.054 (1.37)	0.054 (1.37)	2 (50)

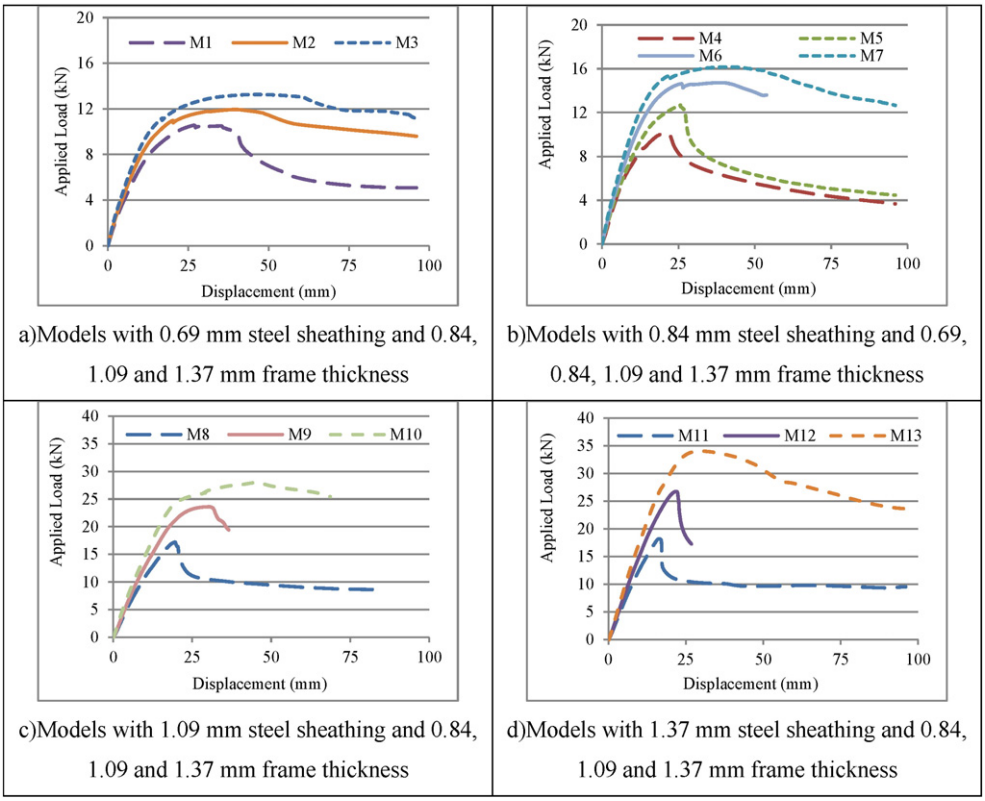

Fig. 17. Lateral load-story displacement response of numerical models.

thickness. In the M2, M3, M6, M7 and M10 models, this ratio is between 1.3 and 2 and the post peak response experience a light negative slop and maintains its strength up to high story displacement. While in the models M1, M4, M5, M8, M11, and M12 this ratio is between 0.82 and 1.22, which caused sudden decrease of strength.

6.2. Tension field and buckling pattern of models

Tension field of steel sheeting of all models at 24 mm displacement is depicted in Fig. 19. As can be seen, in models with the same steel sheeting thickness, the tension field of specimens and the resulted stresses rise with increasing the frame thickness, meaning that in models with weaker frames, the capacity of the walls is governed by the studs' strength.

Since, buckling of studs is governing the post peak response of models, the stud-buckling pattern at the end of analysis are presented in Fig. 19. The buckling of studs in models M1, M4, M5, M8, M11 and M12 are very severe (local buckling of flanges and lateral buckling) that caused to sudden decrease in the lateral strength (Fig. 17). On the contrary, no significant buckling pattern is observed in studs of models M3, M6, M7 and M10 because of using thicker frame members. On the other hand, the location of stud buckling moves upward with increasing the boundary elements' thickness due to growing the steel sheeting participation in wall strength.

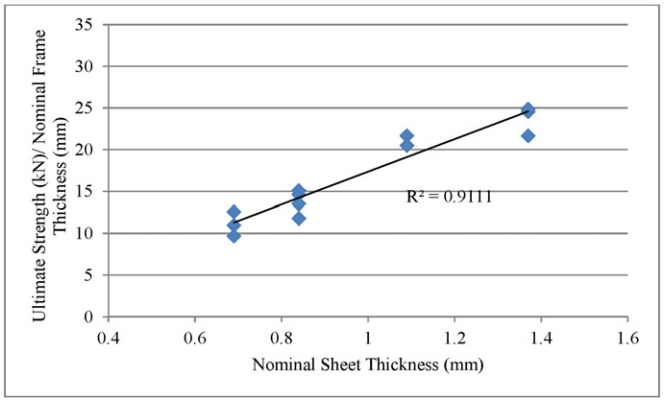

Fig. 18. ratio of ultimate strength of simulated models to frame thickness vs. steel sheeting thickness.

7. Conclusion

In this research, six CFS shear wall with one and two side steel sheeting are tested under reversed cyclic loading, also thirteen numerical models are investigated using Finite Element Method to

Table 6
Secant stiffness and ultimate strength of simulated models.

	Ultimate strength (kN)	Secant stiffness (kN/mm)	Ratio of nominal frame thickness to steel sheathing thickness	Nominal sheet thickness (in) & (mm)	Nominal frame thickness (in) & (mm)
M1	10.56	0.784	1.22	0.027 (0.69)	0.033 (0.84)
M2	11.94	0.906	1.59	0.027 (0.69)	0.043 (1.09)
M3	13.25	1.029	2	0.027 (0.69)	0.054 (1.37)
M4	10.09	0.893	0.82	0.033 (0.84)	0.027 (0.69)
M5	12.67	0.966	1	0.033 (0.84)	0.033 (0.84)
M6	14.72	1.121	1.3	0.033 (0.84)	0.043 (1.09)
M7	16.15	1.261	1.64	0.033 (0.84)	0.054 (1.37)
M8	17.21	1.169	0.77	0.043 (1.09)	0.033 (0.84)
M9	23.61	1.363	1	0.043 (1.09)	0.043 (0.84)
M10	21.95	1.666	1.26	0.043 (1.09)	0.054 (1.37)
M11	18.19	1.282	0.61	0.054 (1.37)	0.033 (0.84)
M12	26.74	1.509	0.8	0.054 (1.37)	0.043 (1.09)
M13	34.04	1.753	1	0.054 (1.37)	0.054 (1.37)

study various steel plates and frame thicknesses. The tested specimens are designed according to Table C2.1–3 of AISI S213-07 and are tested without imposing axial force. Table C2.1–3 of AISI S213-07 is based on Serrette 1997 experimental results. The failure modes that were reported by Serrette include rupture at the edge of the sheeting and stud local buckling in some specimens. While, in the present study the results revealed that other failure modes are possible to occur. Therefore, if the capacity of brittle failure modes governs the performance of the shear wall, the ductility and system overstrength factor will be lower than the ASCE 7–10 values and it should be considered in design procedure.

Overall, both experimental and numerical results indicated that the response of steel plate sheathed CFS frames is highly depends on the ratio of boundary element thickness to steel sheet thickness and the axial capacity of boundary elements.

From experimental part of investigation:

- Based on AISI S213 [3] the available shear strength of two-sided steel-sheathed walls is cumulative. Whereas, based on experimental specimens, it concluded that the response of two sides sheathed CFS shear walls increases (more than twice the strength of one side steel plate sheathed) if the boundary elements are strong enough to sustain

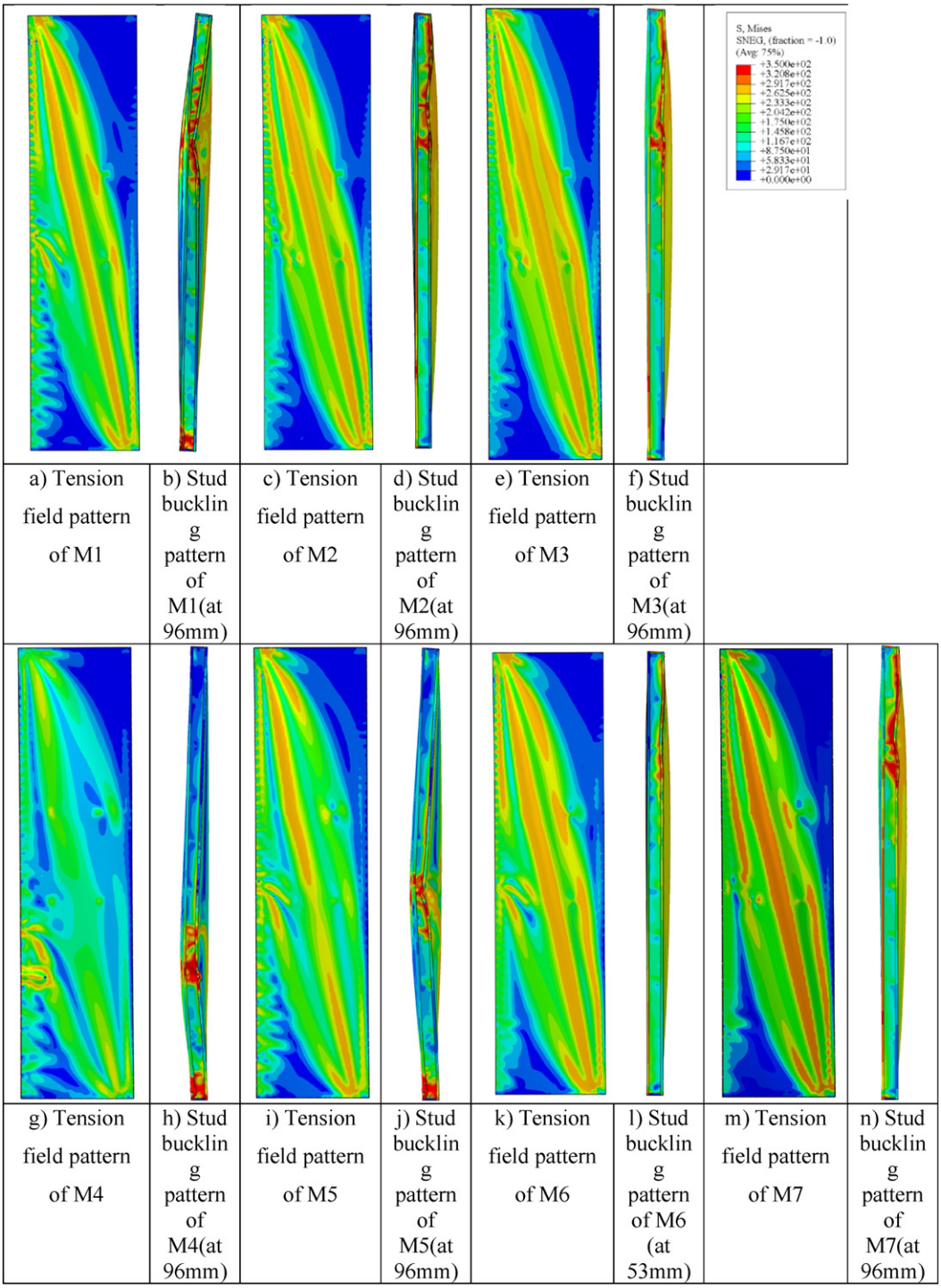

Fig. 19. Tension field pattern of steel sheeting at 24 mm displacement and Stud buckling pattern at end of analysis.

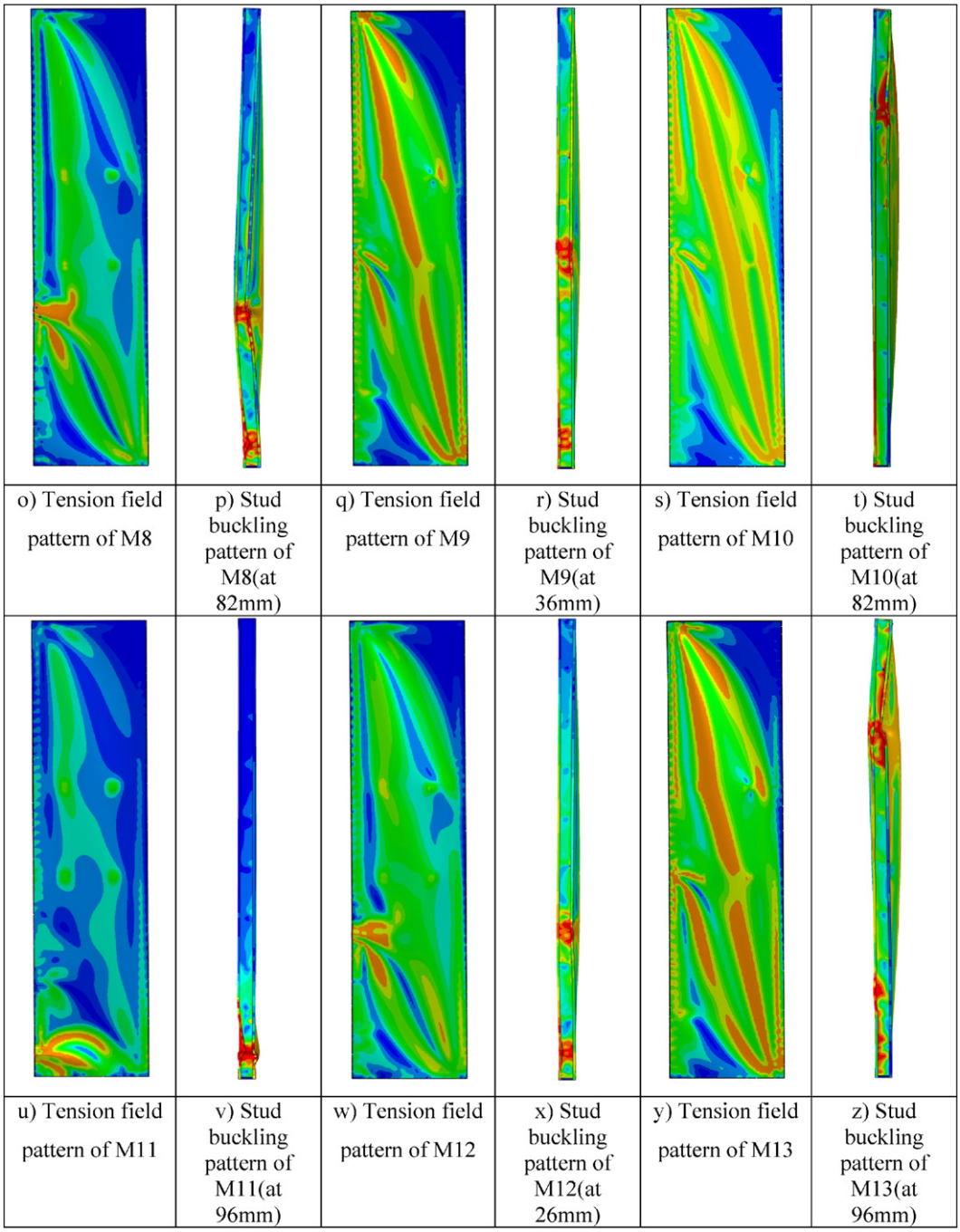

Fig. 19 (*continued*).

the imposed axial forces. Based on the experimental results, in the two side steel sheathed specimens with stud thickness to steel sheeting thickness ratio more than or equal to 2, the available shear strength of wall increase up to twice the strength of one-sided wall. Otherwise, using two-sided shear walls yield to decrease the structural performance of shear wall.

- Although the results of these tests are not adequate for concluding about structural characteristics, based on the results of tested specimens, the response modification factor (R) driven from specimens with weak boundary elements are around 5 which is significantly lower than the specified value in ASCE 7–10. While the response modification factor of specimens with strong boundary elements are about 7 and is the same as the ASCE 7–10 value.
- The average overstrength factor (Ω_0) of specimens shows relatively good agreement with the ASCE 7–10 with the average of 2.08.

From numerical part of investigation:

- The steel sheeting thickness and the ratio of ultimate strength to frame thickness has a linear relationship.
- The influence of stud's axial capacity in ultimate strength becomes smaller with increasing the frame thickness.
- The post peak behavior of investigated models indicates that the post peak negative slope of models are highly depend on the ratio of nominal frame thickness to steel sheet thickness. In models with ratio of nominal frame thickness to steel sheeting thickness higher than 1.3, decrease in post peak strength up to 60 mm lateral

displacement is around 20%, while, In models with ratio of nominal frame thickness to steel sheeting thickness lower than 1.3, decrease in post yield strength up to 60 mm lateral displacement is around 65%.
- Increasing the boundary elements' thickness leads to growing the steel sheeting participation in wall strength and shifts the location of stud buckling from lower regions of the wall to upper regions.

Acknowledgments

We would like to express our gratitude to all those who gave us the possibility to complete this research. The assistance of Building and Housing Research Center (BHRC) structural laboratory staff, including Mr. Nooshabadi and Mr. Khalili is kindly acknowledged. We have furthermore to thank Iranian Society of LSF structures, Tiva Engineering group, and Sazin group for supplying the needed materials.

References

[1] International Code Council, International building code, 2011, ICC, Country Club Hills, Ill, 2012.
[2] ASCE 7-10, Minimum Design Loads for Buildings and Other Structures, American Society of Civil Engineers, Washington, DC, 2010.
[3] AISI S213, North American Standard for Cold-Formed Steel Framing–Lateral Design, American Iron and Steel Institute, Washington DC, 2007.
[4] R.L. Serrette, Additional Shear Wall Values for Light Weight Steel Framing, Report No. LGSRG-1-97, Santa Clara University, Santa Clara, CA, 1997.
[5] C. Yu, Steel Sheet Sheathing Options for Cold-Formed Steel Framed Shear Wall Assemblies Providing Shear Resistance, Report No. UNT-G76234, American Iron and Steel Institute, Washington, DC, 2007.
[6] J. Ellis, Shear Resistance of Cold-Formed Steel Framed Shear Wall Assemblies Using CUREE Test Protocol, Simpson Strong-Tie Co., Inc., 2007
[7] C. Yu, Steel Sheet Sheathing Options for Cold-Formed Steel Framed Shear Wall Assemblies Providing Shear Resistance, Report No. UNT-G70752, American Iron and Steel Institute, Washington, DC, 2009.
[8] Nisreen Balh, Colin A. Rogers, Development of Canadian Seismic Design Provisions for Steel Sheathed Shear Walls, American Iron and Steel Institute, Washington, DC, 2010.
[9] A. Shakibanasab, N.K.A. Attari, M. Salari, A statistical and experimental investigation into the accuracy of capacity reduction factor for cold-formed steel shear walls with steel sheathing, J. Thin-Walled Struct. 77 (2014) 56–66.
[10] M.R. Javaheri-Tafti, H.R. Ronagh, F. Behnamfar, P. Memarzadeh, An experimental investigation on the seismic behavior of cold-formed steel walls sheathed by thin steel plates, J. Thin-Walled Struct. 80 (2014) 66–79.
[11] S. Mohebbi, R. Mirghaderi, F. Farahbod, Sabbagh A. Bagheri, Experimental work on single and double-sided steel sheathed cold-formed steel shear walls for seismic actions, J. Thin-Walled Struct. 91 (2015) 50–62.
[12] Cheng Yu, Yujie Chen, Detailing recommendations for 1.83 m wide cold-formed steel shear walls with steel sheathing, J. Constr. Steel Res. 67 (2011) 93–101.
[13] Xingxing Wang, Jihong Ye, Reversed cyclic performance of cold-formed steel shear walls with reinforced end studs, J. Constr. Steel Res. 113 (2015) 28–42.
[14] Mehran Zeynalian, H.R. Ronagh, Seismic performance of cold formed steel walls sheathed by fibre-cement board panels, J. Constr. Steel Res. 107 (2015) 1–11.
[15] ABAQUS, user's Manual—Version 6.10-1, Hibbit, Karlsson & Sorenson, Pawtucket, RI, 2010.
[16] ASTM A370, A370–06 Standard Test Methods and Definitions for Mechanical Testing of Steel Products, American Society for Testing and Materials, West Conshohocken, PA, 2006.
[17] ASTM A1003/A1003M-11, Standard Specification for Steel Sheet, Carbon, Metallic- and Nonmetallic-Coated for Cold-Formed Framing Members, American Society for Testing and Materials, West Conshohocken, PA, 2011.
[18] ASTM E2126, Standard Test Methods for Cyclic (Reversed) Load Test for Shear Resistance of Vertical Elements of the Lateral Force Resisting Systems for Buildings, American Society for Testing and Materials, West Conshohocken, PA, 2007.
[19] ASCE 41-13, Seismic Evaluation and Retrofit of Existing Buildings, American Society of Civil Engineers, Washington, DC, 2013.
[20] N.M. Newmark, W.J. Hall, Earthquake Spectra and Design, Earthquake Engineering Research Institute, El Cerrito, CA, 1982.